Archives of Biochemistry and Biophysics 755 (2024) 109982

Contents lists available at ScienceDirect

Archives of Biochemistry and Biophysics

journal homepage: www.elsevier.com/locate/yabbi

Brief communication

Glucotoxicity is mediated by cytoplasmic distribution of RAP1 in pancreatic β-cells

A. Deręgowska [a,*], N. Tomaszek [a], P. Cuch [a], K. Kozioł [a], O. Kaniuka [b], M. Sabadashka [b], Yu Bandura [b], N. Sybirna [b]

[a] Institute of Biotechnology, College of Natural Sciences, University of Rzeszow, Pigonia 1, 35-310, Rzeszow, Poland
[b] Department of Biochemistry, Ivan Franko National University of Lviv, 1, Universytetska St., 79000, Lviv, Ukraine

ARTICLE INFO

Keywords:
RAP1
Pancreatic β-cells
Diabetes mellitus
High glucose treatment

ABSTRACT

Diabetes mellitus (DM) is a group of chronic metabolic disorders characterized by persistent hyperglycemia. In our study, we analyzed the level and location of RAP1 changes in the development of β-cell dysfunction induced by glucotoxicity. We employed three pancreatic β-cell lines, namely INS-1, 1.2B4, and NIT-1, as well as a streptozotocin-induced diabetes rat model. We demonstrate that after high glucose treatment, RAP1 is increased, probably through induction by AKT, allowing RAP1 to shuttle from the nucleus to the cytoplasm and activate NF-κB signaling. Furthermore, non-enzymatic post-translational modifications of RAP1, such as advanced glycation end products and carbonylation may affect the function of RAP1, such as activation of the NF-κB signaling. Taken together, we showed that RAP1 is a new player in the mechanism of glucotoxicity in pancreatic β-cells.

1. Introduction

Diabetes mellitus (DM) is a group of metabolic disorders characterized by hyperglycemia over a prolonged period of time resulting from inadequate insulin secretion, insulin resistance, or excessive glucagon secretion [1]. Chronic hyperglycemia causes glucose toxicity and unbalanced redox homeostasis, and in consequence non-enzymatic post-translational protein modifications (nePTMs), such as advanced glycation end products (AGEs) and carbonylation. nePTMs of proteins can lead to protein dysfunction like progressive loss of their biological functions, protein-protein interactions, or incorrect localization in the cell. Moreover, nePTM-modified proteins may become resistant to proteolysis and accumulate inside cells generating aggregates [2,3]. The accumulation of damaged or abnormally modified proteins is amplified in various chronic diseases, such as DM, and has been suggested to be promising diagnostic and prognostic biomarkers for the clinical management of DM [4].

Mammalian RAP1 (Repressor/activator protein 1), also known as TERF2IP (Telomeric repeat-binding factor 2 interaction protein), is characterized by its pleiotropic function, as it is a part of the shelterin complex, which participates in telomere maintenance [5], as well as playing important roles in the regulation of cell homeostasis, including cell metabolism [6–8], inflammation [9], oxidative stress [10] and DNA damage response [11]. However, the functions and mechanisms of RAP1 regulation in DM have not been extensively studied, suggesting the need for further research.

In the present study, we have investigated the effects of the glucotoxic environment on the level of RAP1, localization in both *in vitro* and *in vivo* pancreatic β-cells models. Moreover, the role of AKT, as well as nePTMs, such as carbonylation and glycation in the regulation of RAP1 levels and localization, and the importance of RAP1 dysfunction in the regulation of NFκB-dependent pathways in pancreatic β-cells in response to long-term glucotoxicity was assessed. The potential implications of the results obtained are discussed.

2. Materials and methods

2.1. Cell lines, glucotoxicity culture conditions and treatments

1.2B4 human pancreatic β-cells: HuP-T3 hybrid cell line (ECACC 10070103) and INS-1832/13 rat insulinoma cell line (#SCC208) were obtained from the Merck KgaA (Darmstadt, Germany), and NIT-1 mouse insulinoma cell line (CRL-2055™) was purchased from ATCC (Manassas, VA, USA). 1.2B4 were cultured in RPMI-1640 medium supplemented with 10% fetal bovine serum (FBS). INS-1 cells were cultured with RPMI-1640 supplemented with 2 mM L-glutamine, 1 mM sodium

---

* Corresponding author.
E-mail address: aderegowska@ur.edu.pl (A. Deręgowska).

https://doi.org/10.1016/j.abb.2024.109982
Received 10 November 2023; Received in revised form 4 March 2024; Accepted 28 March 2024

pyruvate, 10 mM HEPES, 0.05 mM β-mercaptoethanol, and 10% FBS. NIT-1 cell line was cultured in DMEM medium supplemented with 10% FBS. All media were supplemented with antibiotic solution (100 U/mL penicillin, 0.1 mg/mL streptomycin, and 0.25 μg/mL amphotericin B) (all from Life Technologies, Carlsbad, CA, USA). Cells were maintained at 37 °C in 5% CO_2 in a humidified incubator. Cells were passaged twice weekly after detachment using trypsin-EDTA (Corning, Tewksbury, MA, USA, 25-053-CI). For experimental glucotoxicity induction cells were cultured in RPMI-1640/DMEM medium supplemented with 16.7 and 25 mM glucose for 24 h, 48 h and 72 h. The medium was replaced every 24 h. In "control" conditions cells were cultured in RPMI-1640/DMEM medium recommended by the manufacturer, and supplemented with 11.2 mM glucose. To determine the role of AKT phosphorylation in the regulation of the nucleo-cytoplasmic distribution of RAP1 during high glucose treatment, the 1.2B4 cells were cultured in RPMI-1640 medium supplemented with 25 mM glucose for 72 h, and treated with 10 nM and 30 nM AKT inhibitor A6730 (Merck KGaA, Darmstadt, Germany), for 48 h and 24 h respectively or DMSO. Control cells were incubated in medium containing 25 mM glucose for 72 h without AKT inhibitor or DMSO. The medium was replaced every 24 h.

2.2. *Experimental animals and induction of diabetes mellitus*

Male Wistar rats, 8–9 weeks old, were used for all experiments (150–180 g in weight). All experimental protocols and study procedures were performed in accordance with the General Principles of Animal Treatment, approved by the First National Congress on Bioethics (Kyiv, Ukraine, 2001), which agreed with the guidelines of Directive 2010/63/EU of the European Parliament on the protection of animals used for scientific purposes and the Law of Ukraine "On Protection of Animals from Cruelty" of February 26, 2006 and approved by the Ethics Committee of Ivan Franko National University of Lviv, Ukraine (Certificate No 22-07-2021 of July 21, 2021). Rats were divided into two groups: streptozotocin (STZ)-induced DM according to the protocols used in modern research [12] and normal untreated control animals (each group included 8–10 animals). The animals were injected with 55 mg STZ dissolved in 10 mM citrate buffer (pH 5.5) per kg of body weight intraabdominally. Blood glycemia was determined after 72 h of STZ injection using the commercially available kit (Filisit Diagnostics, Kyiv, Ukraine). The experimental animals were sacrificed two weeks after induction of diabetes.

2.3. *Cell viability counting*

Necrosis was assessed using a trypan blue dye exclusion assay. Briefly, cells were incubated for 5 min with 0.4% trypan blue and then automatically scored using the TC10™ Automated Cell Counter (Bio-Rad, Hercules, CA, USA).

2.4. *Whole-cell protein extraction, nuclear-cytoplasmic protein extraction and Western blotting*

The cytoplasmic and nuclear extracts were isolated using the NE-PER Nuclear and Cytoplasmic Extraction Reagent Kit (Thermo Fisher Scientific, Waltham, MA, USA) according to the manufacturer's instructions. Whole-cell protein extraction and Western blotting protocols were used as described comprehensively in Ref. [13]. The following primary and secondary antibodies were used: anti-RAP1 (1:1000, #5433, Cell Signaling Technology, Danvers, MA, USA), *anti*-phospho-AKT (Ser473) (1:1000, #4060), *anti*-phospho-AKT (Ser473) (1:1000, 44-621G) (AKT inhibition experiment), *anti*-AKT (1:1000. #4691), *anti*-LC3-I/LC3-II (1:1000, PA1-16931), *anti*-p62 (1:1000, PA5-27247), *anti*-DNP (1:500, MAB2223), anti-AGE (1:1000, AB9890), anti-goat IgG (1:20,000, AP106P), anti-rabbit IgG (1:20,000, #7074 S), anti-mouse IgG (1:20,000, #7076 S) (Thermo Fisher Scientific, Waltham, MA, USA, Merck KGaA, Darmstadt, Germany, and Cell Signaling Technology, Danvers, MA, USA). The membranes were stripped in 62.5 mM Tris-HCl buffer (pH 6.8) containing 2% SDS and 100 mM β-mercaptoethanol for 20 min at 50 °C and reprobed with β-actin antibody (1:40,000, A3854, Merck KGaA, Darmstadt, Germany) to confirm equal protein loading. Densitometry measurements of the bands were performed using ImageJ software (https://imagej.nih.gov/ij/). The data represent the relative density normalized to β-actin. For the analysis of the phosphorylation status of AKT, the ratios of phosphorylated forms to AKT were considered.

2.5. *RAP1 immunoprecipitation*

Immunoprecipitation of RAP1 was performed using Dynabeads Protein G (#10007D, Life Technologies, Carlsbad, CA, USA) according to the manufacturer's instructions. Briefly, 1.5 mg of magnetic beads were incubated with 5 μl of RAP1 antibody (1:1000, #5433, Cell Signaling Technology, Danvers, MA, USA) for 10 min with rotation at RT and then incubated with 100 μg of protein lysate for 60 min with rotation at RT. After washing with Binding and Washing buffer, the Dynabeads-antibody complex was isolated using a magnetic holder, and the supernatant was collected. The RAP1 protein eluent was used for the Western blot-based analysis of nePTM-RAP1 modifications (advanced glycation end products and carbonylation).

2.6. *RAP1 carbonylation*

RAP1 carbonylation was evaluated after RAP1 immunoprecipitation and SDS-PAGE electrophoresis. The gel was electroblotted onto a PVDF membrane. The membrane was washed twice in TBS-T for 5 min, then incubated in 0.1 mg/ml DNPH dissolved in 2 M HCl for 5 min, washed twice in 2 M HCl for 5 min, five times in methanol for 2 min and three times in TBS-T for 1 min. The membranes were then incubated for 1 h at RT in 1% BSA blocking solution and then western blot-based analysis of DNP levels using the *anti*-DNP antibody (1:500, MAB2223, Merck KGaA, Darmstadt, Germany) was performed. For the negative control, the membranes were incubated without DNPH.

2.7. *Advanced glycation end products of RAP1*

The glycation of RAP1 was evaluated after RAP1 immunoprecipitation and western blot-based analysis of AGE levels using the anti-AGE antibody (1:1000, AB9890, Merck KGaA, Darmstadt, Germany).

2.8. *Protein aggregation assay*

Protein aggregate levels were determined using the PROTEOSTAT® Protein aggregation assay (ENZ-51023, Enzo, Farmingdale, NY, USA) was performed according to the manufacturer's instructions. Protein aggregation is presented in relative fluorescence units (RFU).

2.9. *Proteasome 20S activity assay*

Proteasome activity was assessed using the 20 S proteasome assay kit according to the manufacturer's instructions (MAK172, Merck KGaA, Darmstadt, Germany). Briefly, 1.4×10^4 INS-1 cells/1.4×10^4 NIT-1 cells/1.2×10^4 1.2B4 cells were seeded in each well of black clear bottom 96-well plates. After overnight incubation at 37 °C, cells were treated with 16.7 and 25 mM glucose for 24, 48, and 72 h. Next, 100 μL of proteasome assay loading solution was added to each well. 96-well plates were incubated in the dark at 37 °C for 5 h, and chymotrypsin-like protease activity associated with the proteasome complex was measured using a Tecan Infinite® M200 (Tecan Group Ltd., Männedorf, Switzerland) at an excitation wavelength of 490 nm and an emission wavelength of 525 nm. Proteasome 20 S activity is presented in relative fluorescence units (RFU).

2.10. Immunofluorescence

Cell fixation and immunostaining were performed as previously reported [14]. The following primary and secondary antibodies were used: anti-insulin (1:200, #3014), anti-RAP1 antibody (1:200, #5433), *anti*-phospho–NF–κB p65 (pSer536) (1:200, MA515181), and the corresponding fluorochrome-conjugated anti-mouse and anti-rabbit antibodies (1:1000, F2761, T2767) (Cell Signaling Technology, Danvers, MA, USA; Thermo Fisher Scientific, Waltham, MA, USA). DNA was visualized using Hoechst 33342 staining. Cell images were acquired using a laser-based confocal imaging and high-content analysis (HCA) system IN Cell Analyzer 6500 H S and quantitative analysis was performed using IN Carta software (Cytiva, Marlborough, MA, USA). The immunofluorescent signals of the proteins analyzed are presented as relative fluorescence units (RFU).

2.11. Immunofluorescence of RAP1 in rat pancreatic paraffin section

Pancreatic tissue was fixed with formalin, embedded in paraffin, and cut into 5-μm-thick sections. The slides were then deparaffinized with xylene and rehydrated by using graded ethanol. Antigen recovery was performed by using microwave heating for 6 min in 0,01 M sodium citrate-hydrochloric acid buffer. The sections were then washed three times in PBS with 0.25% Triton X-100 (PBS-T), blocked on with 2%

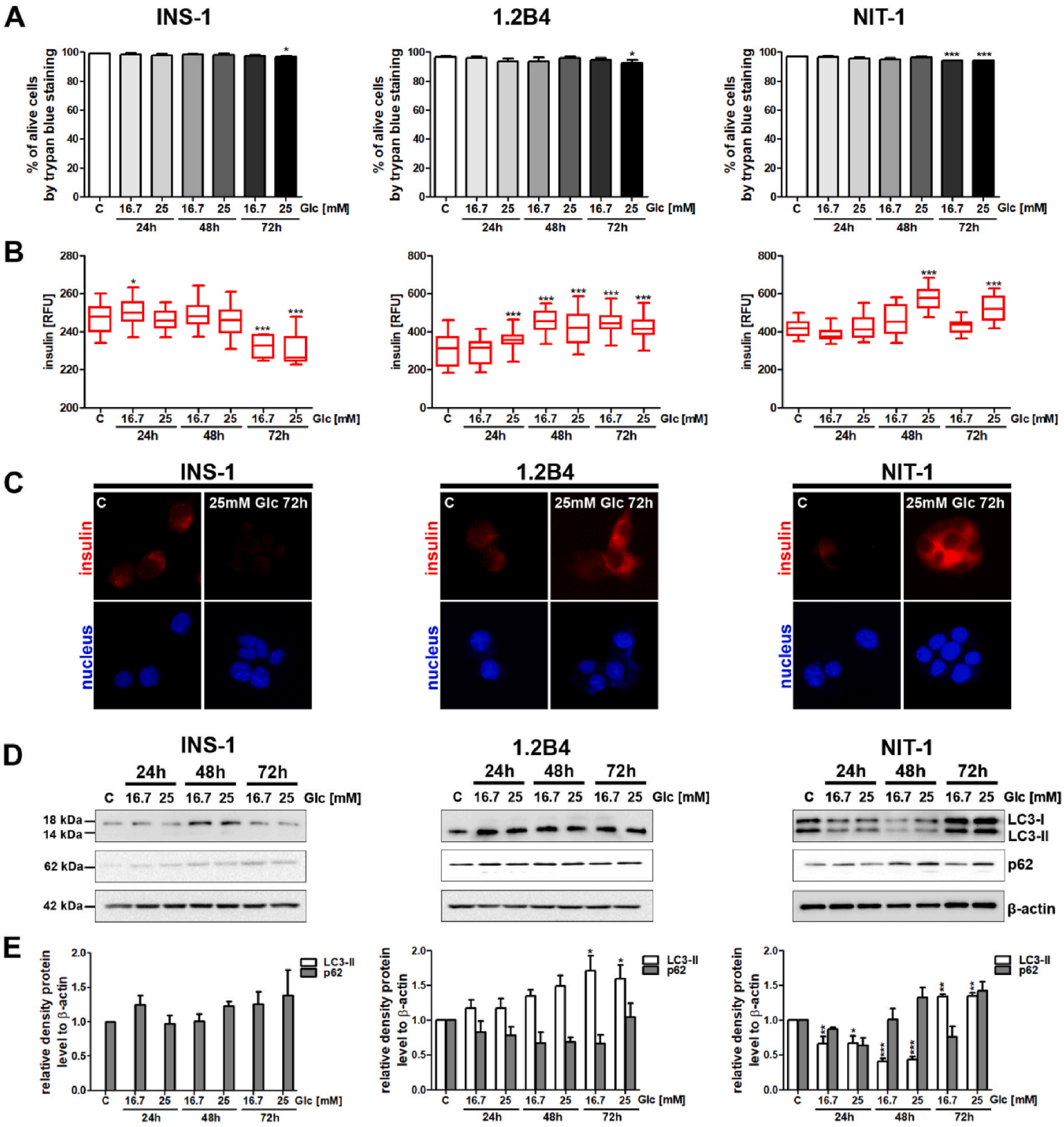

Fig. 1. Characteristics of prolonged exposure of *in vitro* pancreatic INS-1, 1.2B4, and NIT-1 β-cells to high glucose concentrations: **A.** Effects of glucotoxicity on β-cells viability was assessed using trypan blue staining after stimulation with various concentrations (16.7, 25 nM) of glucose for 24 h, 48 h and 72 h. Bars indicate SD, n = 3, ***p < 0.001, *p < 0.05 compared to control cells (C) (ANOVA and Dunnett's a posteriori test); **B.** Insulin levels are expressed as relative fluorescence units (RFU). Box and whisker plots are shown, n = 3, ***p < 0.001, *p < 0.05 compared to C (ANOVA and Dunnett's a posteriori test); **C.** Insulin immunostaining (red), representative microphotographs are shown, objective 20×, nucleus staining (blue). **D-E.** Western blot analysis of LC3-I/-II and p62. β-actin was used as a loading control. Values in the bar graph are presented as the mean ± SD, n = 3, ***p < 0.001, **p < 0.01, *p < 0.05 compared to control cells (C) (ANOVA and Dunnett's a posteriori test); Glc – glucose; C – control cells incubated in medium containing 11.2 mM glucose.

bovine serum albumin in PBS-T for 30 min at room temperature, and washed twice in PBS-T. The samples were then incubated with primary antibody (RAP1, 1:100, #5433, Cell Signaling Technology, Danvers, MA, USA) at 4 °C overnight, followed by incubation with secondary antibody (1:1000, T2767, Thermo Fisher Scientific, Waltham, MA, USA) for 1 h at room temperature. DNA was visualized using DAPI and then analyzed using an Olympus BX61 fluorescence microscope equipped with a DP72 CCD camera and Olympus CellF software (Olympus, Warsaw, Poland). The QuPath software (https://qupath.github.io/) was used to analyze the protein localization.

2.12. *Statistical analysis*

Statistically significant differences between control and glucose-stimulated cells were performed in GraphPad Prism 6.07 software (GraphPad Software, Inc., La Jolla, CA, USA) by one-way ANOVA and with Dunnett's multiple comparison test. Differences between control and diabetes mellitus samples were analyzed using a non-parametric Students' t-test and Mann–Whitney post-test. *P*-values of <0.05 were considered significant.

3. Results and discussion

3.1. *Effects of high glucose on cell viability, insulin content and autophagy activation in INS-1, 1.2B4 and NIT-1 β-cells*

Since hyperglycemia is the metabolic hallmark of DM, we first investigated the effects of high glucose concentrations (16.7 mM and 25 mM) on INS-1, 1.2B4 and NIT-1 cell lines after 24 h, 48 h, and 72 h, in terms of cell viability, insulin content, and autophagy activation. The trypan blue exclusion assay revealed that glucotoxicity does not have a negative impact on survival of INS-1, 1.2B4 and NIT-1 cells (Fig. 1A). However, a discreet reduction effect was observed at 72 h in all analyzed cell lines, which was the result of high confluence in long-term cultures. Our data are consistent with previously published results [15,16].

Therefore, we tested whether prolonged high-glucose stimulation could lead to impaired insulin secretion (Fig. 1B–C). 1.2B4 cells grown with high glucose showed the most noticeable response than those cultured with 11.2 mM glucose among all cell lines tested. NIT-1 cells showed increased insulin secretion at 25 mM concentrations for 48 h and 72 h compared to control cells. Interestingly, INS-1 cells showed lower insulin secretion after 72 h of high glucose stimulation than control cells. However, long-term cultured rat INS-1 cells showed a trend to lose the differentiated β-cells phenotype, including the insulin response to glucose due to the dominance of poor glucose-responsive cells in culture or the change in the expression of GSIS-responsible genes [17,18]. Similarly, in NIT-1 mice cultured for 48 h in 5.6 mM DMEM, 11.6 mM RPMI-1640, and 25 mM DMEM, there were no differences in insulin secretion caused by the adaptation of the cells to a wide range of glucose concentrations [19]. In human islets, only a small fraction of heterogeneous β-cells contributes to the majority of insulin secretion. Furthermore, the architecture of human islets and cellular contacts has been largely attributed to insulin secretion [20].

Since autophagy is an essential process for pancreatic β-cell homeostasis and plays a protective role for β-cells function in a high-glucose diet [21], we have analyzed whether autophagy can be activated in our experimental model. Activation of autophagy in β-cells was measured by LC3-I/LC3-II and p62 protein levels (Fig. 1D–E). High glucose increased autophagy in 1.2B4 and in NIT-1 after 72 h treatment compared to control cells incubated in a medium containing 11.2 mM glucose. No signs of autophagy activation were detected after high glucose stimulation at each time point of the INS-1 line, according to previous reports [21]. The expression of p62 under high glucose conditions did not change statistically in all β-cells lines compared to control cells. Altered β-cells autophagy has been accused in patients with type 2 diabetes, and in obese diabetic rodents [21], and autophagy triggered by endoplasmic reticulum stress (ER stress) has been postulated as an alternative degradation process of misfolded proteins, such as proinsulin [22].

3.2. *High glucose-stimulation have effects on cytoplasmic localization of the RAP1 protein, and AKT phosphorylation level*

Since the RAP1 protein, in addition to its telomeric role, is also described as a transcriptional repressor/activator of genes involved in cell metabolism [6–8], in the next step, we investigated the effects of high glucose stimulation of the *in vitro* β-cell lines model and STZ-induced DM *in vivo* model of on RAP1 level and localization (Fig. 2). Western blot analyses of total protein lysates from pancreatic β-cell lines demonstrated that RAP1 was increased in INS-1 cells at both all-time points and glucose concentrations analyzed. For 1.2B4 an increase in RAP1 level was observed after 72 h stimulation with high glucose, while no significant differences were observed for the NIT-1 cell line (Fig. 2A–B). Furthermore, RAP1 protein levels in the nucleus and cytoplasm were evaluated by immunofluorescence staining (Fig. 2C–D) and Western blot (Fig. 2E–F). Immunofluorescence staining revealed that exposure of β-cells to high glucose conditions at 48 h and 72 h significantly increased the cytoplasmic content of RAP1 in both rodent cell lines, while in the human 1.2B4 cell line an increase in the cytoplasmic level of RAP1 was observed after 72 h of stimulation with 25 mM glucose. The increase in the cytoplasmic fraction was accompanied by a decrease in the nuclear fraction in 1.2B4 and 16.7 mM glucose-stimulated for 24 h and 25 mM for 48 h in NIT-1 cells. The exception was the INS-1 line, in which an increase in the nuclear fraction of RAP1 was observed after 72 h of stimulation with 25 mM glucose. Western blot analysis showed similar trends. Furthermore, STZ-induced DM induction resulted in the loss of nuclear RAP1 with an increase in the cytoplasmic fraction (Fig. 2G–H). These observations suggest that RAP1 may be related to the development of β-cell dysfunction induced by glucotoxicity. Previous findings of RAP1 deficiency mice showed signs of metabolic dysfunction, such as glucose intolerance, liver steatosis, accumulation of abdominal fat, obesity, and significant transcriptional changes of metabolic genes [6,7], while Rap1 (mutated, unable to bind to telomeres) knock-in mice are characterized by increased fasting blood glucose levels and body weight, activation of pro-inflammatory chemokines, and spontaneous tumour incidence [23].

DM-associated impaired glucose metabolism was associated with AKT activation [31,32], so we decided to analyze the level of the phosphorylated form of AKT in Ser-473 (Fig. 2A–B). Similarly to previous reports, which indicated that glucose activates AKT in insulinoma cells [33], we found glucose-activated AKT after 48 and 72 h of high glucose stimulation for both INS-1 and NIT-1 cells, while 72 h of high glucose stimulation for 1.2B4 cells. Furthermore, high levels of phosphorylated AKT were found to be positively correlated with the total level of RAP1, as well as with cytoplasmic RAP1. In the study by Lee et al., it was shown that AKT1 kinase is one of the proteins involved in the phosphorylation of telomeric proteins, including RAP1 [34]. To further investigate whether the AKT signaling pathway regulated RAP1 localization, 1.2B4 cells were treated with the AKT inhibitor A6730. Western blot results showed that while treated with the AKT inhibitor, the protein level of cytoplasmic RAP1 decreased, while no changes were observed at the protein level of nuclear RAP1 (Fig. 2I–J). These results led us to hypothesise that AKT activation would be necessary to maintain the cytoplasmic pool of RAP1 under high glucose conditions in pancreatic β-cells.

Considering that RAP1 was found to shuttle between the nucleus and the cytoplasm and modulate NF-κB signaling through p65 phosphorylation [9], in the next step, it was evaluated whether the tested conditions of glucotoxicity lead to RAP1-dependent activation of the NF-κB pathway (Fig. 2C–D). Previous studies reported that in lung adenocarcinoma A549 cell line RAP1 deletion attenuates phosphorylation of p65 at Ser-536 in the nuclear fraction [24]. In the case of INS-1 cells, 24 h of

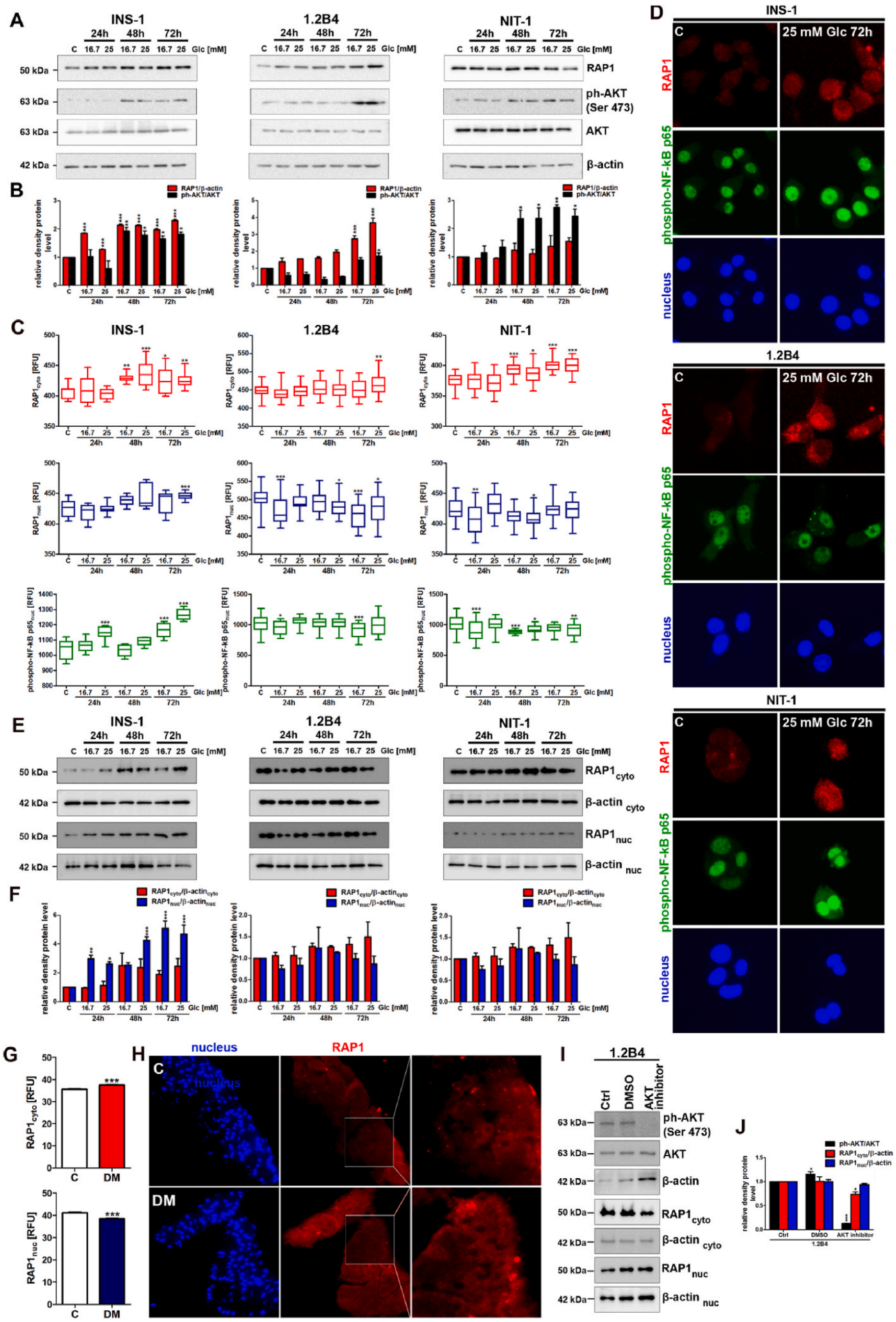

Fig. 2. Abundance and localization of RAP1 protein in high glucose-stimulated *in vitro* pancreatic β-cells model and streptozotocin-induced diabetic rats: **A-B.** Western blot analysis and densitometry quantification of RAP1 and phosphorylated (ph-AKT) form of AKT in high glucose-stimulated INS-1, 1.2B4 and NIT-1 cells. The ph-AKT value was measured as a ratio of ph-AKT to AKT. β-actin was used as a loading control. Bars indicate SD, $n = 3$, $***p < 0.001$, $**p < 0.01$, $*p < 0.05$ compared to control cells (C) (ANOVA and Dunnett's a posteriori test). **C-D.** RAP1 immunofluorescence (red), and phosporylated–NF–κB p65 (green).Box and whisker plots are shown, nuclear/cytoplasmic RAP1 levels are presented as relative fluorescence units (RFU), $n = 3$, $***p < 0.001$, $**p < 0.01$, $*p < 0.05$ compared to control cells (C) (ANOVA and Dunnett's a posteriori test). Representative microphotographs are shown, objective 20×, nucleus staining (blue). **E-F.** Western blot analysis and densitometry quantification of nuclear/cytoplasmic RAP1 levels. β-actin was used as a loading control. Bars indicate SD, $n = 3$, $***p < 0.001$, $**p < 0.01$, $*p < 0.05$ compared to control cells (C) (ANOVA and Dunnett's a posteriori test). **G-H.** RAP1 immunofluorescence (red) in pancreatic tissue of control rats and animals with experimental DM cells. Cell nuclei were visualized by DAPI. Bars indicate mean and SEM. Statistical analysis was performed with the non-parametric Students' t-test and Mann–Whitney post-test,$***p < 0.001$. **I-J.** The protein expression levels of the nuclear/cytoplasmic RAP1 and phosphorylated (ph-AKT) form of AKT in 1.2B4 cells treated with the AKT inhibitor (A6730) or DMSO. The ph-AKT value was measured as a ratio of ph-AKT to AKT. β-actin was used as a loading control. Bars indicate SD, $n = 3$, $***p < 0.001$, $*p < 0.05$ compared to control cells (Ctrl) (ANOVA and Dunnett's a posteriori test); Glc – glucose, C – control cells incubated in medium containing 11.2 mM glucose, cyto – cytoplasm, nuc – nucleus, Ctrl – control cells incubated in medium containing 25 mM glucose for 72 h without AKT inhibitor or DMSO.

incubation in 25 mM glucose, as well as 72 h of incubation in both 16.7 and 25 mM glucose resulted in an increased level of p65 phosphorylation at Ser-536.These results are in agreement with previous studies that indicated that high glucose (33.3 mM) induces NF-κB activation in INS-1 cells [25]. However, significantly down-regulated NF-κB p65 phosphorylation at Ser-536 for NIT-1 cells, and selectively for 1.2B4 cells after high glucose stimulation compared to control cells was observed. Further, NF-κB activation enhances RAP1 production [9]. It should also be considered that RAP1-dependent activation of NF-κB p65 may be mediated by phosphorylation at p65 sites, different from that we analyzed, as described in retinal cells, where high glucose upregulated phosphorylation of p65 at Thr-254, Ser-276, Thr-435, Ser-468 and Ser-529 [26]. Interestingly, to date, most studies on the role of NF-κB are inconclusive and have focused mainly on the role of NF-κB signaling in peripheral tissues in the pathogenesis of DM [27]. An anti-apoptotic role of NF-κB in murine insulinoma cells was described [28], on the other hand, the pro-apoptotic role of NF-κB in NOD mice [29], and rat insulinoma cells were reported [25]. The influence of NF-κB signal-transduction pathways on cell viability or function is highly dependent on exposure of β-cells to inflammatory cytokines [29].

3.3. Chronic exposure of pancreatic β-cells to high glucose affects glycation, carbonylation of RAP1, and proteasome 20s activity, but had no effect on protein aggregation level

Impaired glucose metabolism and antioxidant defence in DM [30] are associated with the occurrence of non-enzymatic post-translational modifications of proteins, such as the formation of advanced glycation end products (AGEs) and carbonylation, which in turn can become more resistant to proteolytic degradation [31,32]. As RAP1 levels increased after exposure to high glucose concentration, we were also interested in whether RAP1 can be selectively glycated and/or carbonylated. We found that in NIT-1 cells high glucose conditions markedly reduced glycated, as well as carbonylated RAP1 in a concentration and time-dependent manner, while in INS-1 and 1.2B4 we found no statistically significant differences compared to control cells (Fig. 3A–B). It suggests that NIT-1 cells have a more efficient process of glycated protein degradation compared to INS-1 or 1.2B4. Furthermore, high glucose-stimulated changes in the level of the glycated or carbonylated form of RAP1 were associated with a decrease in nuclear localization of NF-κB suggesting that nePTMs may interfere with RAP1 function, such as activation of the NF-κB signalling. It should be noted that glycation and carbonylation of RAP1 and their role in the regulation of RAP1 upon high glucose stimulation have not been previously documented. The accumulation of AGE-and/or carbonylated-mediated protein aggregates may be observed in cells with proteasome dysfunctions [31,32]. No increase in protein aggregation level was observed under high glucose conditions in all β-cell lines tested (Fig. 3C). These results indicate that high glucose simulation does not influence the accumulation of damaged proteins, such as RAP1. According to the 20 S proteasome activity, cell lines can be ranked as follows: INS-1>1.2B4>NIT-1 (Fig. 3D). A significant increase in 20 S proteasome activity was

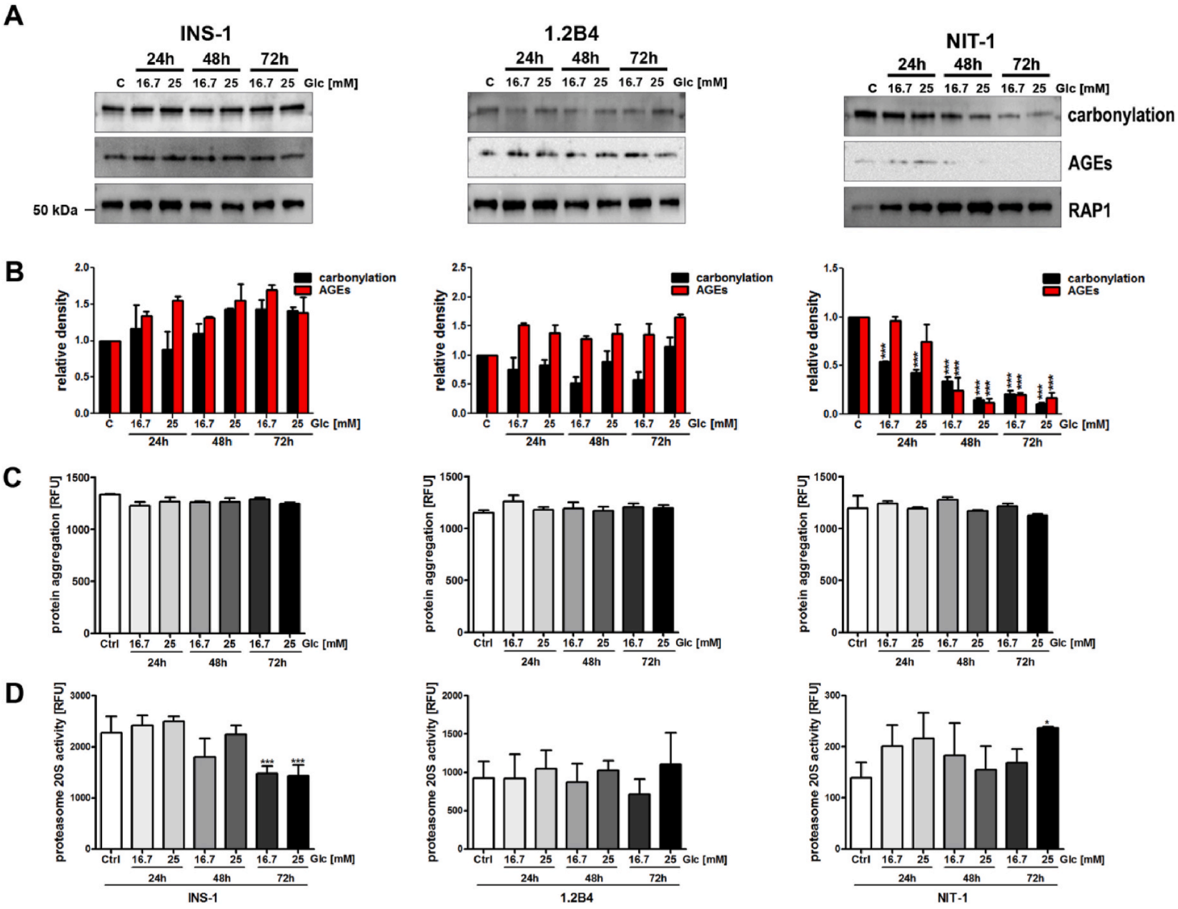

Fig. 3. High glucose-mediated non-enzymatic post-translational modifications of RAP1, protein aggregation and proteasome activity in pancreatic β-cells: **A-B.** Western blot analysis of advanced glycated end products (AGEs) and carbonylation levels after RAP1 immunoprecipitation in INS-1, 1.2B4 and NIT-1 cells. Quantitative analysis is provided. Bars indicate SD, AGE: n = 3; carbonylation: n = 2, ***p < 0.001, **p < 0.01, *p < 0.05 compared to control cells (C). **C.** Protein aggregation, evaluated using a dedicated fluorescence-based kit, is presented in relative fluorescence units (RFU). Bars indicate SD, n = 3. **D.** Proteasome activity assessed by measuring the proteolytic activity of the 20 S core unit using a fluorogenic substrate. Bars indicate SD, n = 3, ***p < 0.001,*p < 0.05 compared to control cells (C) (ANOVA and Dunnett's a posteriori test); Glc – glucose, C – control cells incubated in medium containing 11.2 mM glucose.

observed in NIT-1 cells after 72 h (25 mM) of glucose exposure compared to control cells, suggesting that under high glucose stimulation, 20 S proteasomes become more active leading to rapid rates of carbonylated and glycated degradation of RAP1. However, a decrease in 20 S proteasome activity was observed in INS-1 cells after 72 h under conditions of high glucose (16.7 and 25 mM). Similar effects were observed in a previous study showing that glucotoxic conditions can alter proteasome activities in the INS-1 rat insulinoma cell line [33].

4. Conclusions

In conclusion, our work integrates RAP1 as a new key player in the mechanism of glucotoxicity in pancreatic β-cells. We report here that an increase in the level of the RAP1 protein in the cytosol fraction occurred in pancreatic β-cells under glucotoxicity conditions and in the rat model of diabetes mellitus, indicating its significance in metabolic diseases associated with hyperglycemia, including DM. RAP1 is upregulated after high glucose stimulation, possibly through induction by AKT, allowing RAP1 to nucleocytoplasmic translocation and activation of NF-κB signaling. It should also be emphasized that in β-cells, non-enzymatic post-translational RAP1 modifications such as glycation and carbonylation do not accumulate in the cell, but are efficiently eliminated by both the ubiquitin–proteasome system and the autophagy system; however, non-enzymatic post-translational RAP1 modifications can alter the function of RAP1, such as activation of the NF-κB signaling. These findings warrant further study on the potential functions of RAP1 in the development of β-cell dysfunction induced by glucotoxicity.

Funding

This work was supported by the National Science Centre of Poland, Miniatura 5, Grant number: 2021/05/X/NZ3/01210 (**A.D.**)

CRediT authorship contribution statement

A. Deręgowska: Conceptualization, Formal analysis, Investigation, Visualization, Writing – original draft, Funding acquisition, Writing – review & editing. **N. Tomaszek:** Formal analysis, Investigation. **P. Cuch:** Formal analysis, Investigation. **K. Kozioł:** Investigation. **O. Kaniuka:** Formal analysis, Investigation, Methodology. **M. Sabadashka:** Formal analysis, Investigation. **Yu Bandura:** Investigation. **N. Sybirna:** Conceptualization, Writing – review & editing.

Declaration of competing interest

We declare that there are no conflicts of interest.

Data availability

Data will be made available on request.

Acknowledgements

The authors thank Maciej Wnuk (University of Rzeszow, Poland) for his help and constructive criticism of the manuscript and thank anonymous reviewers for providing valuable comments on the manuscript.

References

[1] D. Tomic, J.E. Shaw, D.J. Magliano, The burden and risks of emerging complications of diabetes mellitus, Nat. Rev. Endocrinol. 18 (2022) 525–539, https://doi.org/10.1038/s41574-022-00690-7.

[2] R. Harmel, D. Fiedler, Features and regulation of non-enzymatic post-translational modifications, Nat. Chem. Biol. 14 (2018) 244–252, https://doi.org/10.1038/nchembio.2575.

[3] N. Chondrogianni, I. Petropoulos, S. Grimm, K. Georgila, B. Catalgol, B. Friguet, T. Grune, E.S. Gonos, Protein damage, repair and proteolysis, Mol. Aspect. Med. 35 (2014) 1–71, https://doi.org/10.1016/j.mam.2012.09.001.

[4] P. Gillery, S. Jaisson, Usefulness of non-enzymatic post-translational modification derived products (PTMDPs) as biomarkers of chronic diseases, J. Proteonomics 92 (2013) 228–238, https://doi.org/10.1016/j.jprot.2013.02.015.

[5] B. Li, S. Oestreich, T. de Lange, Identification of human Rap1, Cell 101 (2000) 471–483, https://doi.org/10.1016/S0092-8674(00)80858-2.

[6] P. Martinez, M. Thanasoula, A.R. Carlos, G. Gómez-López, A.M. Tejera, S. Schoeftner, O. Dominguez, D.G. Pisano, M. Tarsounas, M.A. Blasco, Mammalian Rap1 controls telomere function and gene expression through binding to telomeric and extratelomeric sites, Nat. Cell Biol. 12 (2010) 768–780, https://doi.org/10.1038/ncb2081.

[7] F. Yeung, C.M. Ramírez, P.A. Mateos-Gomez, A. Pinzaru, G. Ceccarini, S. Kabir, C. Fernández-Hernando, A. Sfeir, Nontelomeric role for Rap1 in regulating metabolism and protecting against obesity, Cell Rep. 3 (2013) 1847–1856, https://doi.org/10.1016/j.celrep.2013.05.032.

[8] Y. Cai, V. Kandula, R. Kosuru, X. Ye, M.G. Irwin, Z. Xia, Decoding telomere protein Rap1: its telomeric and nontelomeric functions and potential implications in diabetic cardiomyopathy, Cell Cycle 16 (2017) 1765–1773, https://doi.org/10.1080/15384101.2017.1371886.

[9] H. Teo, S. Ghosh, H. Luesch, A. Ghosh, E.T. Wong, N. Malik, A. Orth, P. de Jesus, A. S. Perry, J.D. Oliver, N.L. Tran, L.J. Speiser, M. Wong, E. Saez, P. Schultz, S. K. Chanda, I.M. Verma, V. Tergaonkar, Telomere-independent Rap1 is an IKK adaptor and regulates NF-kappaB-dependent gene expression, Nat. Cell Biol. 12 (2010) 758–767, https://doi.org/10.1038/ncb2080.

[10] M.J. Swanson, M.E. Baribault, J.N. Israel, N.S. Bae, Telomere protein RAP1 levels are affected by cellular aging and oxidative stress, Biomed Rep 5 (2016) 181–187, https://doi.org/10.3892/br.2016.707.

[11] E. Khattar, V. Tergaonkar, Role of Rap1 in DNA damage response: implications in stem cell homeostasis and cancer, Exp. Hematol. 90 (2020) 12–17, https://doi.org/10.1016/j.exphem.2020.08.009.

[12] W. Wang, D. Bai, C. Wu, H. Li, X. Xie, W. Ji, J. Gao, A protocol for constructing a rat wound model of type 1 diabetes, JoVE (2023) 64914, https://doi.org/10.3791/64914.

[13] A. Deregowska, M. Pepek, K. Pruszczyk, M.M. Machnicki, M. Wnuk, T. Stoklosa, Differential regulation of telomeric complex by BCR-ABL1 kinase in human cellular models of chronic myeloid leukemia-from single cell analysis to next-generation sequencing, Genes 11 (2020), https://doi.org/10.3390/genes11101145.

[14] D. Bloniarz, J. Adamczyk-Grochala, A. Lewinska, M. Wnuk, The lack of functional DNMT2/TRDMT1 gene modulates cancer cell responses during drug-induced senescence, Aging 13 (2021) 15833–15874, https://doi.org/10.18632/aging.203203.

[15] W. El-Assaad, J. Buteau, M.-L. Peyot, C. Nolan, R. Roduit, S. Hardy, E. Joly, G. Dbaibo, L. Rosenberg, M. Prentki, Saturated fatty acids synergize with elevated glucose to cause pancreatic β-cell death, Endocrinology 144 (2003) 4154–4163, https://doi.org/10.1210/en.2003-0410.

[16] S. Srinivasan, E. Bernal-Mizrachi, M. Ohsugi, M.A. Permutt, Glucose promotes pancreatic islet β-cell survival through a PI 3-kinase/Akt-signaling pathway, Am. J. Physiol. Endocrinol. Metabol. 283 (2002) E784–E793, https://doi.org/10.1152/ajpendo.00177.2002.

[17] M. Skelin, Pancreatic beta cell lines and their applications in diabetes mellitus research, ALTEX (2010) 105–113, https://doi.org/10.14573/altex.2010.2.105.

[18] K.-G. Park, K.-M. Lee, H.-Y. Seo, J.-H. Suh, H.-S. Kim, L. Wang, K.-C. Won, H.-W. Lee, J.-Y. Park, K.-U. Lee, J.-G. Kim, B.-W. Kim, H.-S. Choi, I.-K. Lee, Glucotoxicity in the INS-1 rat insulinoma cell line is mediated by the orphan nuclear receptor small heterodimer partner, Diabetes 56 (2007) 431–437, https://doi.org/10.2337/db06-0753.

[19] Q. Xu, S.Y. Chen, L.D. Deng, L.P. Feng, L.Z. Huang, R.R. Yu, Antioxidant effect of mogrosides against oxidative stress induced by palmitic acid in mouse insulinoma NIT-1 cells, Braz. J. Med. Biol. Res. 46 (2013) 949–955, https://doi.org/10.1590/1414-431X20133163.

[20] A. Wojtusciszyn, M. Armanet, P. Morel, T. Berney, D. Bosco, Insulin secretion from human beta cells is heterogeneous and dependent on cell-to-cell contacts, Diabetologia 51 (2008) 1843–1852, https://doi.org/10.1007/s00125-008-1103-z.

[21] Q. Sheng, X. Xiao, K. Prasadan, C. Chen, Y. Ming, J. Fusco, N.N. Gangopadhyay, D. Ricks, G.K. Gittes, Autophagy protects pancreatic beta cell mass and function in the setting of a high-fat and high-glucose diet, Sci. Rep. 7 (2017) 16348, https://doi.org/10.1038/s41598-017-16485-0.

[22] Z. Yin, C. Pascual, D. Klionsky, Autophagy: machinery and regulation, Microb Cell 3 (2016) 588–596, https://doi.org/10.15698/mic2016.12.546.

[23] A.J. Stock, R.A. McDevitt, C. Puligilla, Y. Wang, Y. Zhang, K. Wang, C. Sun, K. G. Becker, E. Lehrmann, W.H. Wood, Y. Gong, M. Aqdas, M.-H. Sung, V. Hoffmann, C. Liu, M. Gorospe, L. Harrington, L. Ferrucci, Y. Liu, Aberrant expression and localization of the RAP1 shelterin protein contribute to age-related phenotypes, PLoS Genet. 18 (2022) e1010506, https://doi.org/10.1371/journal.pgen.1010506.

[24] L. Xiao, X. Lan, X. Shi, K. Zhao, D. Wang, X. Wang, F. Li, H. Huang, J. Liu, Cytoplasmic RAP1 mediates cisplatin resistance of non-small cell lung cancer, Cell Death Dis. 8 (2017) e2803, https://doi.org/10.1038/cddis.2017.210, e2803.

[25] Q. Zhang, Y. Xue, B. Zhu, J. Li, J. Sha, S. Li, [High glucose induces INS-1 cell apoptosis by activating nuclear factor-κB], Nan Fang Yi Ke Da Xue Xue Bao 30 (2010) 2307–2309.

[26] H. Shi, E.A. Berger, Characterization of site-specific phosphorylation of NF- κ B p65 in retinal cells in response to high glucose and cytokine polarization, Mediat. Inflamm. 2018 (2018) 1–15, https://doi.org/10.1155/2018/3020675.

[27] L. Catrysse, G. Van Loo, Inflammation and the metabolic syndrome: the tissue-specific functions of NF-κB, Trends Cell Biol. 27 (2017) 417–429, https://doi.org/10.1016/j.tcb.2017.01.006.

[28] I. Chang, S. Kim, J.Y. Kim, N. Cho, Y.-H. Kim, H.S. Kim, M.-K. Lee, K.-W. Kim, M.-S. Lee, Nuclear factor κB protects pancreatic β-cells from tumor necrosis factor-α-mediated apoptosis, Diabetes 52 (2003) 1169–1175, https://doi.org/10.2337/diabetes.52.5.1169.

[29] S. Kim, I. Millet, H.S. Kim, J.Y. Kim, M.S. Han, M.-K. Lee, K.-W. Kim, R.S. Sherwin, M. Karin, M.-S. Lee, NF-κB prevents β cell death and autoimmune diabetes in NOD mice, Proc. Natl. Acad. Sci. U.S.A. 104 (2007) 1913–1918, https://doi.org/10.1073/pnas.0610690104.

[30] V. Poitout, R.P. Robertson, Glucolipotoxicity: fuel excess and β-cell dysfunction, Endocr. Rev. 29 (2008) 351–366, https://doi.org/10.1210/er.2007-0023.

[31] I. Dalle-Donne, G. Aldini, M. Carini, R. Colombo, R. Rossi, A. Milzani, Protein carbonylation, cellular dysfunction, and disease progression, J. Cell Mol. Med. 10 (2006) 389–406, https://doi.org/10.1111/j.1582-4934.2006.tb00407.x.

[32] J.-L. Wautier, A.M. Schmidt, Protein glycation: a firm link to endothelial cell dysfunction, Circ. Res. 95 (2004) 233–238, https://doi.org/10.1161/01.RES.0000137876.28454.64.

[33] C. Broca, E. Varin, M. Armanet, C. Tourrel-Cuzin, D. Bosco, S. Dalle, A. Wojtusciszyn, Proteasome dysfunction mediates high glucose-induced apoptosis in rodent beta cells and human islets, PLoS One 9 (2014) e92066, https://doi.org/10.1371/journal.pone.0092066.